LETTER

doi:10.1038/nature17966

Seasonality of temperate forest photosynthesis and daytime respiration

R. Wehr[1], J. W. Munger[2], J. B. McManus[3], D. D. Nelson[3], M. S. Zahniser[3], E. A. Davidson[4], S. C. Wofsy[2] & S. R. Saleska[1]

Terrestrial ecosystems currently offset one-quarter of anthropogenic carbon dioxide (CO_2) emissions because of a slight imbalance between global terrestrial photosynthesis and respiration[1]. Understanding what controls these two biological fluxes is therefore crucial to predicting climate change[2]. Yet there is no way of directly measuring the photosynthesis or daytime respiration of a whole ecosystem of interacting organisms; instead, these fluxes are generally inferred from measurements of net ecosystem–atmosphere CO_2 exchange (NEE), in a way that is based on assumed ecosystem-scale responses to the environment. The consequent view of temperate deciduous forests (an important CO_2 sink) is that, first, ecosystem respiration is greater during the day than at night; and second, ecosystem photosynthetic light-use efficiency peaks after leaf expansion in spring and then declines[3], presumably because of leaf ageing or water stress. This view has underlain the development of terrestrial biosphere models used in climate prediction[4,5] and of remote sensing indices of global biosphere productivity[5,6]. Here, we use new isotopic instrumentation[7] to determine ecosystem photosynthesis and daytime respiration[8] in a temperate deciduous forest over a three-year period. We find that ecosystem respiration is lower during the day than at night—the first robust evidence of the inhibition of leaf respiration by light[9–11] at the ecosystem scale. Because they do not capture this effect, standard approaches[12,13] overestimate ecosystem photosynthesis and daytime respiration in the first half of the growing season at our site, and inaccurately portray ecosystem photosynthetic light-use efficiency. These findings revise our understanding of forest–atmosphere carbon exchange, and provide a basis for investigating how leaf-level physiological dynamics manifest at the canopy scale in other ecosystems.

Much of what has been inferred about the behaviour of ecosystem photosynthesis, or 'gross ecosystem production' (GEP, defined as ecosystem-scale photosynthesis minus photorespiration), and 'daytime ecosystem respiration' (DER) in forests derives from eddy covariance measurements of their difference, denoted 'net ecosystem exchange' (NEE). NEE measurements have greatly advanced our understanding of carbon-cycle processes in terrestrial ecosystems, but the behaviours of GEP and DER have remained uncertain because eddy covariance does not distinguish one process from the other. In standard practice, a hypothesized response of GEP and/or DER to light, water, and/or temperature is used to make that distinction and thereby partition NEE into GEP and DER. For example, the oldest, simplest, and still most commonly adopted hypothesis is that DER follows the same function of air or soil temperature as does night-time ecosystem respiration[12,13], which is directly observable as night-time NEE. Another common partitioning hypothesis is that DER follows a function of air temperature of the same form found to apply to night-time NEE (but not necessarily with the same parameter values), while GEP follows a saturating function of photosynthetically active radiation (PAR) of the same form found to apply to individual leaves[14].

To date there has been no means of testing these partitioning hypotheses, but they are nevertheless used in hundreds of studies each year. The most popular partitioning algorithm[13] alone has been cited more than 800 times since its debut in 2005, and similar methods have been explored since the onset of long-term eddy covariance measurements[12]. The patterns and environmental responses of GEP and DER obtained from such methods have been used to design and evaluate terrestrial biosphere models for estimating large-scale biosphere–atmosphere interactions and predicting climate change[4,5]. Partitioning has also been applied to a range of ecosystems to evaluate various remote sensing indices that may enable aircraft and satellite measurements of regional and global biosphere productivity but have contrasting seasonal patterns[5,6,15,16]. And partitioning has been used to investigate ecosystem light-use efficiency and water-use efficiency, and to evaluate related production efficiency models intended to estimate regional and global biosphere productivity[17,18].

The general pattern observed via standard partitioning of NEE in temperate deciduous forests is that DER peaks or plateaus shortly after leaf expansion[3,19], one to two months ahead of the peak in belowground respiration[19]. Meanwhile, the ecosystem photosynthetic light-use efficiency peaks shortly after leaf expansion and then gradually declines through the growing season—as might occur because of leaf ageing or water stress—until autumnal senescence[3].

To investigate the behaviour of GEP and DER, we partitioned three growing seasons of subhourly NEE measurements at the Harvard Forest into GEP and DER, on the basis of simultaneous eddy covariance measurements of the stable carbon isotopic composition (that is, $^{13}C/^{12}C$) of NEE[7]. Our isotopic flux partitioning (IFP) algorithm (see Methods) exploits the fact that GEP and DER have $^{13}C/^{12}C$ signatures[8] that are almost always distinguishable in subhourly NEE given the high precision (Extended Data Fig. 1) of our recently developed infrared laser spectrometer[7] (see also Extended Data Fig. 2). We focus on comparisons with the most common standard partitioning algorithm[13]; comparisons with the partitioning method that incorporates a photosynthetic light-response function[14] are broadly similar and can be found in the Methods.

Our analysis indicates that daytime ecosystem respiration differed fundamentally from standard predictions that were based on night-time NEE and temperature[13] (Fig. 1): DER was only about half as large as night-time NEE in the first half of the growing season (June–July), but was roughly equal to night-time NEE in the second half (August–September). As belowground respiration typically varies by less than 10% between daytime and night-time at this site[20], the large discrepancy between daytime and night-time ecosystem respiration in the first half of the growing season suggests inhibition of leaf respiration by light, known as the Kok effect[9]. Such inhibition has been found to occur at the leaf level in many plant species[10], including tree species[11]

[1]Department of Ecology and Evolutionary Biology, University of Arizona, Tucson, Arizona 85721, USA. [2]School of Engineering and Applied Sciences and Department of Earth and Planetary Sciences, Harvard University, Cambridge, Massachusetts 02138, USA. [3]Aerodyne Research Inc., Billerica, Massachusetts 01821, USA. [4]Appalachian Laboratory, University of Maryland Center for Environmental Science, Frostburg, Maryland 21532, USA.

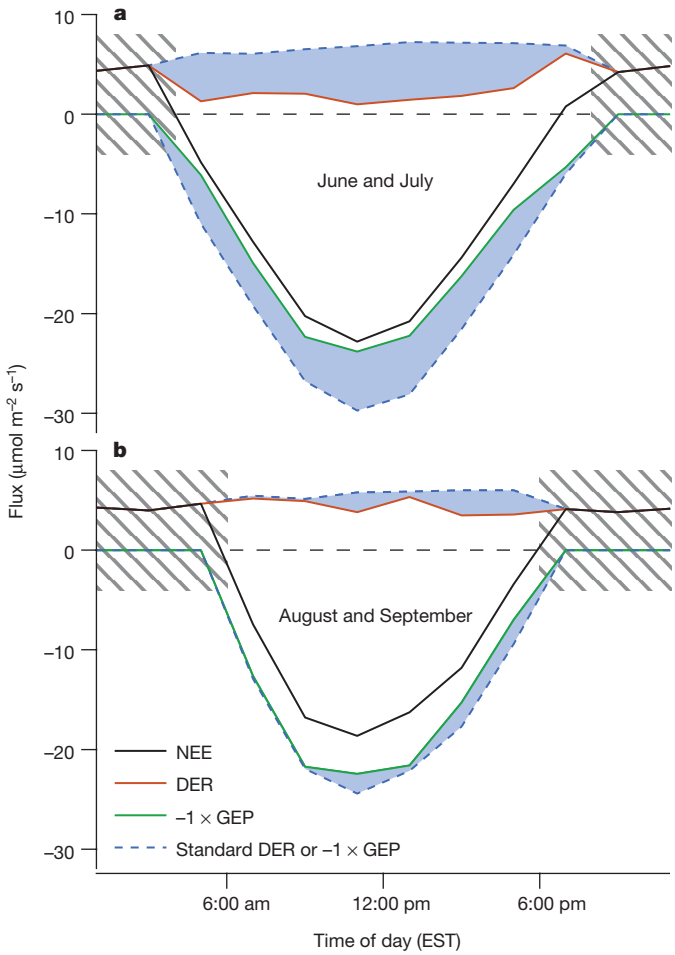

Figure 1 | Composite diel cycles show that photosynthesis and daytime respiration at the Harvard Forest are less than predicted in the first half of the growing season. a, **b**, Fluxes in the tower's relatively homogeneous and well sampled southwest quadrant, averaged across the three years, 2011–2013, for June to July (**a**) and August to September (**b**). Differences from the results of standard partitioning for the same data are shaded in blue. Lines connect means for each 2-hour bin ($20 \leq n \leq 94$). Partitioning is done for daylight periods only; GEP is set to zero in the dark (hatched areas).

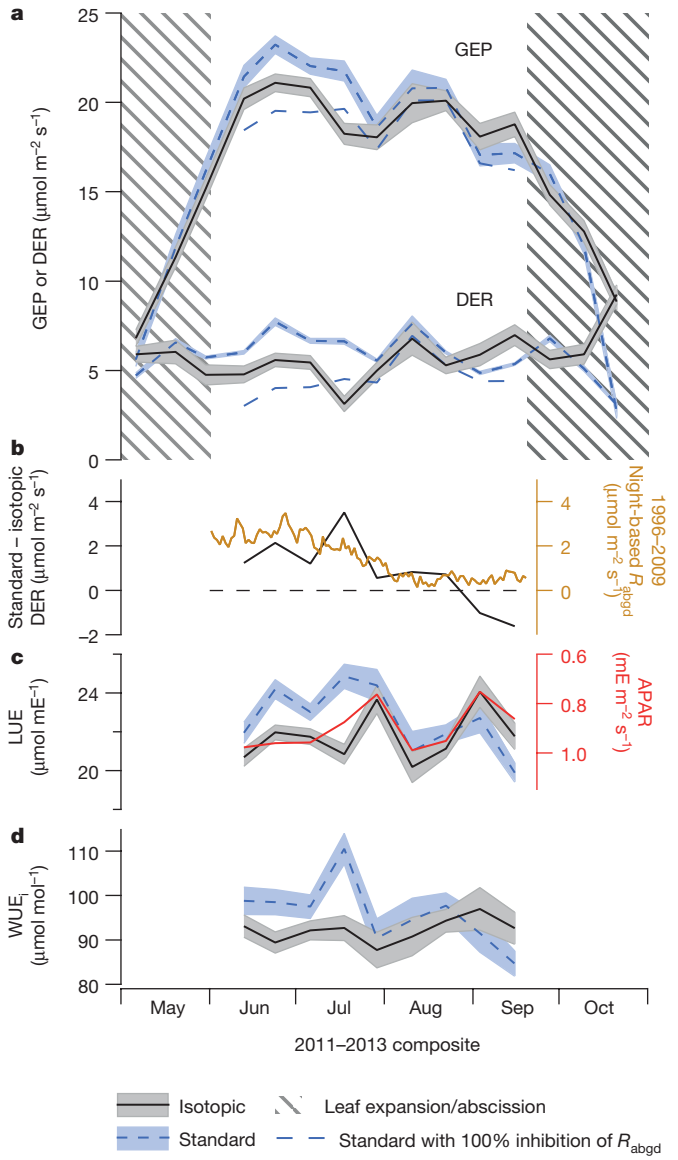

Figure 2 | Composite seasonal cycles of GEP and DER indicate strong inhibition of aboveground respiration by light and sustained photosynthetic efficiency. Results from isotopic partitioning, standard partitioning, and standard partitioning adjusted for 100% inhibition of aboveground respiration by light (see Methods), across all forest quadrants. **a**, GEP and DER. **b**, Discrepancy between standard and isotopic partitioning (black line), with the gold line showing the 1996–2009 mean seasonal pattern of aboveground respiration (R_{abgd}) estimated from soil chambers and night-time NEE[19]. **c**, Light-use efficiency (LUE; isotopic and standard partitioning), with absorbed photosynthetically active radiation (APAR) inverted in red. **d**, Intrinsic water-use efficiency (WUE_i). Lines connect means over all daylight hours for each 12-day bin; pale bands show standard errors of the means calculated from variability within each bin ($64 \leq n \leq 431$). Bands are omitted from the 100%-inhibition lines for clarity. Hatched areas indicate periods of leaf expansion and abscission.

(although we know of no published studies in red oak, which dominates our site). We therefore asked: what would cause inhibition of leaf respiration to occur during the first half of the growing season only, and is the magnitude of the discrepancy consistent with the overall respiration budget?

Previous work[19] at this site on the seasonal patterns of aboveground and belowground respiration—a multiyear synthesis of more than 100,000 flux tower and soil chamber observations—suggests that in June, at night, aboveground respiration typically accounts for more than 50% of total ecosystem respiration, but that this proportion declines to about 10% in August (Fig. 2b, gold line). June–July is the period in which leaves are still thickening after expansion[15,16] and are presumably continuing growth respiration associated with that thickening, which might explain the elevated night-time respiration of the canopy. (In contrast, night-time canopy respiration is roughly stable from June through to September at a nearby conifer-dominated site[19].) We infer that aboveground respiration is strongly inhibited by light during the day at our site, causing DER to be about half as large as night-time ecosystem respiration in June–July but almost equal to night-time ecosystem respiration in August–September (Fig. 1). Near-complete inhibition of leaf respiration by light has been reported for individual leaves of some species[10], and so both the seasonal pattern and the magnitude of the discrepancy between daytime and night-time ecosystem respiration are consistent with a plausible ecosystem-scale Kok effect.

Standard partitioning calculates DER from night-time NEE without accounting for any inhibition of respiration by light, and so the seasonally varying discrepancy between night-time and daytime ecosystem respiration (as determined by isotopic partitioning) corresponds to a similar, seasonally varying discrepancy between standard and isotopic estimates of DER (Fig. 2a, b). However, standard partitioning—and therefore the discrepancy between standard and isotopic partitioning—can be complicated by horizontal heterogeneity in ecosystem

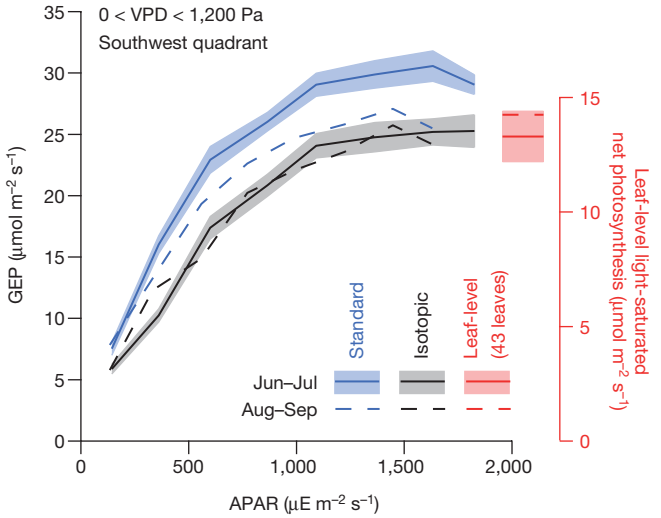

Figure 3 | The ecosystem-scale light-response curve is invariant over the season. Responses of GEP (from isotopic and standard partitioning) to APAR, in June–July and August–September (before leaf abscission), averaged across all three years, for vapour pressure deficits (VPDs) of between 0 Pa and 1,200 Pa, in the flux tower's southwest quadrant. Lines connect means for each APAR bin, and pale bands show standard errors of the means calculated from variability within each bin ($14 \leq n \leq 63$). Also shown (right-hand axis) are the leaf-level light-saturated net photosynthesis rates (that is, net leaf CO_2-uptake rates) reported for the years 1991 to 1992 in ref. 26, based on 43 red oak leaves in mid July and 44 red oak leaves in late August; the small increase from mid July to late August was also reported for red maple leaves in ref. 26. Bands are omitted from the August–September curves for clarity.

respiration surrounding the flux measurement tower. Standard partitioning uses all night-time fluxes in a 4- or 6-day time window to predict DER for each individual daytime flux measurement. The night-time fluxes typically correspond to many different sectors of the forest, according to the winds; but the individual daytime flux being partitioned corresponds to one particular sector. Therefore, standard partitioning effectively averages across sectors, underestimating DER for high-respiration sectors and overestimating it for low-respiration sectors[8]. Moreover, if the winds differ systematically between day and night, standard DER predictions can be further biased. At our site, ecosystem respiration was more than two times larger to the northwest of the flux measurement tower than it was to the southwest[8], and the day-versus-night wind biases in our data set were such that the June–July discrepancy between standard and isotopic estimates of DER is understated when averaging across all sectors of the forest (as in Fig. 2), but exaggerated when averaging only within the southwest quadrant (as in Fig. 1). Without these sampling biases, the standard method would have overestimated DER by about 100% in June–July (see Methods).

We have thus far described only the period between the completion of leaf expansion and the onset of autumnal senescence (June–September). Prior to leaf expansion, aboveground respiration already constitutes more than half of night-time ecosystem respiration, probably because of respiration associated with bud and leaf development, branch elongation, and wood production[19]. In this period, we found that daytime and night-time ecosystem respiration were roughly equal, so that the standard and isotopic partitioning methods agreed (Fig. 2a). This result is expected, as respiration should be inhibited by light only in photosynthesizing tissues.

The revised seasonal pattern in DER corresponds to a new seasonal pattern in GEP, because DER and GEP are constrained to sum to the measured NEE in both partitioning methods. Whereas standard partitioning suggested a gradual decline in the response of GEP to absorbed photosynthetically active radiation (APAR) through the growing season, isotopic partitioning showed that the response of GEP to APAR was stable between the completion of leaf expansion and the onset of autumnal senescence (Fig. 3). Neither GEP (Fig. 2a) nor the canopy light-use efficiency (LUE, being GEP/APAR) (Fig. 2c) determined by isotopic partitioning exhibited the pronounced early-season peak that typifies standard estimates at this site and in temperate forests more generally[3]. Compared with isotopic partitioning, and aside from the directional sampling biases mentioned above, standard partitioning overestimated GEP by about 25% in June–July.

Qualitatively, the observed saturating response of GEP to APAR (Fig. 3) and the resulting negative correlation between LUE and APAR (Fig. 2c) make physiological sense for three reasons. First, as the amount of light increases, the photosynthetic apparatus of a leaf becomes increasingly limited by other factors, such as CO_2 supply[21]. Second, cloudy or hazy conditions cause the amount of light to decline but the remaining light to be more diffuse and therefore spread more evenly among the canopy leaves, strongly increasing assimilation by otherwise shaded leaves but only mildly reducing assimilation by otherwise sunlit, light-saturated leaves[22]. Third, high-light conditions tend to be associated with drier air, which can lower LUE by inducing stomatal restriction of the CO_2 supply. Quantitatively, the observed seasonal-scale relationship between isotopically determined LUE and APAR ($r^2 = 0.75$, $P = 0.002$ between the completion of leaf expansion and the onset of abscission; Fig. 2c and Extended Data Fig. 3) is expected, in the sense that it is consistent with relationships obtained from both standard and isotopic partitioning at shorter timescales (Extended Data Fig. 4). In contrast, LUE predicted by standard partitioning did not yield any significant seasonal-scale correlation with APAR ($r^2 = 0.07$, $P = 0.39$) (Fig. 2c and Extended Data Fig. 3). There would indeed be such a correlation were it not for the June–July LUE peak, which we argue is an artefact arising because standard partitioning does not capture the inhibition of leaf respiration by light.

Another common metric of photosynthetic efficiency is canopy-intrinsic water-use efficiency (WUE_i)[23], which is the ratio of carbon gained by photosynthesis (GEP) to water lost by transpiration (E_T), controlling for the water-vapour mole fraction gradient between the inside of the leaves and the air (Δw). Thus, $WUE_i = 1.6 \times \Delta w \times GEP/E_T$ (the factor of 1.6 in this definition accounts for the fact that water vapour diffuses 1.6 times more quickly than CO_2). We found that WUE_i was more stable throughout the growing season than is predicted by standard partitioning (Fig. 2d), implying a stable relationship between canopy stomatal conductance and GEP.

In some forests, LUE is believed to decline before the onset of senescence owing to water stress[24]. Some plants exhibit a decline in LUE as leaves age[25]. In our forest, however, leaf-level gas-exchange measurements indicate little or no decline in photosynthetic capacity for our site-dominant tree species before senescence[15,26] (Fig. 3, red lines). Moreover, our observations show that the soil water content increased, and the atmospheric vapour pressure deficit decreased, from July to September (Extended Data Fig. 5): that is, water stress was decreasing throughout that period. Thus, LUE should not be expected to decline before senescence at our site, in accordance with our partitioning results. Indeed, given existing literature on the leaf-level Kok effect[9–11], and on the seasonal patterns of aboveground respiration[19] and leaf-level photosynthetic capacity at our site[15,26], the seasonal patterns of DER and GEP derived from isotopic partitioning appear more consistent with present knowledge than do those obtained by standard partitioning.

Our findings suggest a need to reappraise standard partitioning methods at other flux tower sites, in other ecosystems, to determine whether the patterns we have observed at the Harvard Forest are common elsewhere. For example, in equatorial Amazonian forests, standard eddy-covariance-based estimates of GEP and LUE increase throughout the dry season. That increase contradicts some model predictions, but is supported by observations of increased leaf flushing at the start of the dry season[27,28]. Our findings, however, point to the possibility that

some of the apparent seasonality in tropical GEP might actually be a partitioning artefact introduced by not accounting for seasonality in (light-inhibited) leaf respiration, with young leaves respiring more (at night), as here.

The empirical understanding of carbon exchange between temperate forests and the atmosphere that underpins efforts to estimate global biosphere productivity[5,6] and to predict climate change[4,5] holds that ecosystem respiration is greater during the day than at night, and that the canopy photosynthetic light-use efficiency gradually declines throughout the growing season. But the strong apparent light-mediated inhibition of canopy respiration and the invariance of the canopy photosynthetic light response found here challenge that understanding. These phenomena also highlight the central role of leaf-level physiological dynamics in ecosystem-scale responses to the environment, and the potential benefit of incorporating more accurate representation of such dynamics into Earth-system models. Our study suggests that ecosystem-scale isotopic flux measurements could provide a general basis for exploring how leaf-level dynamics play out in ecosystems of varying composition and phenology around the world.

Online Content Methods, along with any additional Extended Data display items and Source Data, are available in the online version of the paper; references unique to these sections appear only in the online paper.

Received 15 September 2015; accepted 23 March 2016.

1. Intergovernmental Panel on Climate Change. *Climate Change 2013: The Physical Science Basis* (Cambridge Univ. Press, 2013).
2. Schimel, D. *et al.* Observing terrestrial ecosystems and the carbon cycle from space. *Glob. Change Biol.* **21,** 1762–1776 (2015).
3. Falge, E. *et al.* Seasonality of ecosystem respiration and gross primary production as derived from FLUXNET measurements. *Agric. For. Meteorol.* **113,** 53–74 (2002).
4. Stöckli, R. *et al.* Use of FLUXNET in the community land model development. *J. Geophys. Res.* **113,** 1–19 (2008).
5. Parazoo, N. C. *et al.* Terrestrial gross primary production inferred from satellite fluorescence and vegetation models. *Glob. Change Biol.* **20,** 3103–3121 (2014).
6. Turner, D. P. *et al.* Scaling gross primary production (GPP) over boreal and deciduous forest landscapes in support of MODIS GPP product validation. *Remote Sens. Environ.* **88,** 256–270 (2003).
7. Wehr, R. *et al.* Long-term eddy covariance measurements of the isotopic composition of the ecosystem–atmosphere exchange of CO_2 in a temperate forest. *Agric. For. Meteorol.* **181,** 69–84 (2013).
8. Wehr, R. & Saleska, S. R. An improved isotopic method for partitioning net ecosystem-atmosphere CO_2 exchange. *Agric. For. Meteorol.* **214–215,** 515–531 (2015).
9. Kok, B. On the interrelation of respiration and photosynthesis in green plants. *Biochim. Biophys. Acta* **3,** 625–631 (1949).
10. Heskel, M. A., Atkin, O. K., Turnbull, M. H. & Griffin, K. L. Bringing the Kok effect to light: a review on the integration of daytime respiration and net ecosystem exchange. *Ecosphere* **4,** 98 (2013).
11. Sun, J. *et al.* Estimating daytime ecosystem respiration to improve estimates of gross primary production of a temperate forest. *PLoS One* **9,** http://dx.doi.org/10.1371/journal.pone.0113512 (2014).
12. Wofsy, S. C. *et al.* Net exchange of CO_2 in a mid-latitude forest. *Science* **260,** 1314–1317 (1993).
13. Reichstein, M. *et al.* On the separation of net ecosystem exchange into assimilation and ecosystem respiration: review and improved algorithm. *Glob. Change Biol.* **11,** 1424–1439 (2005).
14. Lasslop, G. *et al.* Separation of net ecosystem exchange into assimilation and respiration using a light response curve approach: critical issues and global evaluation. *Glob. Change Biol.* **16,** 187–208 (2010).
15. Dillen, S. Y., Phillips, N., de Beeck, M. O., Hufkens, K. & Buonanduci, M. Agricultural and forest meteorology. *Agric. For. Meteorol.* **160,** 60–68 (2012).
16. Keenan, T. F. *et al.* Tracking forest phenology and seasonal physiology using digital repeat photography: a critical assessment. *Ecol. Appl.* **24,** 1478–1489 (2014).
17. Tang, X. *et al.* How is water-use efficiency of terrestrial ecosystems distributed and changing on Earth? *Sci. Rep.* **4,** 7483 (2014).
18. Yuan, W. *et al.* Global comparison of light use efficiency models for simulating terrestrial vegetation gross primary production based on the LaThuile database. *Agric. For. Meteorol.* **192–193,** 108–120 (2014).
19. Giasson, M. A. *et al.* Soil respiration in a northeastern US temperate forest: a 22-year synthesis. *Ecosphere* **4,** 140 (2013).
20. Savage, K., Davidson, E. A. & Tang, J. Diel patterns of autotrophic and heterotrophic respiration among phenological stages. *Glob. Change Biol.* **19,** 1151–1159 (2013).
21. De Pury, D. G. G. & Farquhar, G. D. Simple scaling of photosynthesis from leaves to canopies without the errors of big-leaf models. *Plant Cell Environ.* **20,** 537–557 (1997).
22. Knohl, A. & Baldocchi, D. D. Effects of diffuse radiation on canopy gas exchange processes in a forest ecosystem. *J. Geophys. Res.* **113,** G02023 (2008).
23. Beer, C. *et al.* Temporal and among-site variability of inherent water use efficiency at the ecosystem level. *Global Biogeochem. Cycles* **23,** GB2018 (2009).
24. Grassi, G., Vicinelli, E., Ponti, F., Cantoni, L. & Magnani, F. Seasonal and interannual variability of photosynthetic capacity in relation to leaf nitrogen in a deciduous forest plantation in northern Italy. *Tree Physiol.* **25,** 349–360 (2005).
25. Constable, G. A. & Rawson, H. M. Effect of leaf position, expansion and age on photosynthesis, transpiration and water use efficiency of cotton. *Funct. Plant Biol.* **7,** 89–100 (1980).
26. Bassow, S. L. & Bazzaz, F. A. How environmental conditions affect canopy leaf-level photosynthesis in four deciduous tree species. *Ecology* **79,** 2660–2675 (1998).
27. Restrepo-Coupe, N. *et al.* What drives the seasonality of photosynthesis across the Amazon basin? A cross-site analysis of eddy flux tower measurements from the Brasil flux network. *Agric. For. Meteorol.* **182–183,** 128–144 (2013).
28. Wu, J. *et al.* Leaf development and demography explain photosynthetic seasonality in Amazon evergreen forests. *Science* **351,** 972–976 (2016).

Acknowledgements This research was supported by the US Department Of Energy (DOE), Office of Science, Terrestrial Ecosystem Science (TES) program (award DE-SC0006741), and the Agnese Nelms Haury Program in Environment and Social Justice at the University of Arizona. Soil chamber data were acquired with the help of K. Savage at the Woods Hole Research Center, under the DOE award. The Harvard Forest Environmental Measurements Site infrastructure is a component of the Harvard Forest Long-Term Ecological Research (LTER) site, supported by the National Science Foundation (NSF), and is additionally supported by the DOE TES program. Below-canopy PAR, soil temperature and soil moisture data were provided by E. Nicoll at the Harvard Forest, supported by the NSF LTER program. OCS data and SIF data were provided by the authors of refs 40 and 41, respectively.

Author Contributions S.R.S. conceived the study. S.R.S. and R.W. designed the study. R.W., J.B.M., D.D.N. and M.S.Z. developed and maintained the spectrometer. R.W. and J.W.M. set up and maintained the instrumentation and conducted the measurements. R.W. analysed the data and wrote the manuscript. R.W. and S.R.S. led the interpretation of the results with input from J.W.M., S.C.W. and E.A.D. All authors contributed to editing the manuscript.

Author Information Reprints and permissions information is available at www.nature.com/reprints. The authors declare no competing financial interests. Readers are welcome to comment on the online version of the paper. Correspondence and requests for materials should be addressed to R.W. (rawehr@email.arizona.edu) or S.R.S. (saleska@email.arizona.edu).

METHODS

Data availability. The measurements used, as well as ancillary site data, are publicly available from the Harvard Forest Data Archive (http://harvardforest.fas.harvard.edu/harvard-forest-data-archive) under records HF209 and HF004. The measurements are also publicly available at ftp://saleskalab.eebweb.arizona.edu/, along with the analysis algorithms used.

Site description. The measurements used here were acquired between May 2011 and October 2013 at the Harvard Forest Environmental Measurements Site[13,29], which is situated in a mostly deciduous temperate forest dominated by red oak and red maple (with some hemlock and red pine) in Massachusetts, USA. Average seasonal cycles of key environmental and forest variables are shown in Extended Data Fig. 5.

Measurements. Acquisition of isotopic fluxes (described previously[7]) was via a recently developed quantum cascade laser spectrometer that measures the isotopic composition of atmospheric CO_2 with unprecedented accuracy and precision. The long-term (>3-year) reproducibility in 100-s measurements by this spectrometer is ± 0.1‰ for $\delta^{13}C$ and ± 0.12‰ for $\delta^{18}O$ (95% confidence interval) (Extended Data Fig. 1) The short term (<3-hour) precision in 100-s measurements—which is the relevant metric for distinguishing isotopic signatures in updrafts and downdrafts and, hence, for using the eddy covariance method—is ± 0.04‰ for $\delta^{13}C$ and ± 0.06‰ for $\delta^{18}O$ (95% confidence interval).

Environmental and forest variables used in this study (Extended Data Fig. 5) include:

Plant area index. This was measured optically across a plot array in the flux tower footprint throughout the growing season (as part of routine site operations), interpolated to our 40-minute time grid, and converted to leaf area index (LAI) as described elsewhere[8]. The period between the completion of leaf expansion and the onset of leaf abscission is defined as the time during which the LAI was greater than 95% of its stable summertime maximum.

Absorbed photosynthetically active radiation (APAR). This is calculated as the difference between above-canopy PAR and below-canopy PAR (that is, neglecting reflection), the latter of which was calculated as the mean of six measurements (using Li-Cor LI-190S quantum sensors mounted 1 metre above the ground) distributed within the flux tower footprint.

Soil temperature. This was calculated as the mean of measurements from eight copper-constantan thermocouples buried 10 cm below the ground surface, distributed within the typical flux tower footprint.

Volumetric soil moisture. This was measured for the depth range 0–30 cm at four locations in the typical flux tower footprint.

Isotopic flux partitioning. Since its original exposition[30], the isotopic partitioning of NEE has been tested in several ecosystems[31–38] but has not been generally adopted owing to instrumental limitations. Motivated by the improvements in field instrumentation described above, we recently extended the theory of isotopic flux partitioning (IFP), and successfully demonstrated its application at the Harvard Forest for the first year of our measurements, quantifying its uncertainties and potential biases[8]. Here we briefly recapitulate our method.

The basic idea of IFP is to determine GEP and DER using their isotopic signatures and the magnitude and isotopic composition of their residual, NEE; in other words, to solve the following set of two mass balance equations for the two unknowns, DER and GEP, where δ^{13}_{NEE}, δ^{13}_{DER}, and δ^{13}_{GEP} describe the ratios (expressed relative to a standard material) of ^{13}C to ^{12}C in NEE, DER, and GEP, respectively:

$$NEE = DER - GEP$$

$$\delta^{13}_{NEE}NEE = \delta^{13}_{DER}DER - \delta^{13}_{GEP}GEP$$

Because the isotopic signature of GEP (that is, δ^{13}_{GEP}) varies substantially during the day, additional equations based on leaf anatomy and biochemistry are used to express the isotopic signature of GEP in terms of GEP itself, chiefly via the canopy-integrated stomatal conductance, determined from heat and water fluxes measured by eddy covariance[8]. In our recently extended theory of isotopic partitioning[8], the two equations above are replaced by a system of six equations in which DER is broken down into foliar and non-foliar respiration, and GEP is broken down into gross photosynthesis and photorespiration. The breakdown is necessary because each of these four processes has its own isotopic signature.

The isotopic signature of non-foliar respiration is the only signature that is measured, by a combination of soil chamber and night-time Keeling plot measurements[8]. This method is weighted strongly to belowground respiration[8]. To the degree that the isotopic signature of non-foliar aboveground respiration differed from that of belowground respiration, our isotopic signature of overall non-foliar respiration would therefore have been in error. However, we showed previously that the partitioning is not very sensitive to that signature: a relatively large 1‰ error in the signature of overall non-foliar respiration leads to an error of just 3% in GEP[8].

Although our IFP algorithm[8] treats foliar and non-foliar respiration separately because of their independent isotopic signatures, the rates of foliar and non-foliar respiration cannot be determined separately from one another with confidence by IFP (at least at present) because neither is directly measurable or predictably related to other variables—as, for example, photorespiration is related to photosynthesis by the photocompensation point (which is measurable) and DER is related to photosynthesis and photorespiration by NEE (which is measurable). In other words, we have enough information to solve the equations for DER but not to apportion DER to foliar and non-foliar sources. The attribution of patterns in DER to patterns in foliar respiration in the main text is therefore based instead on comparison to belowground respiration measured by soil chambers.

For the purposes of the calculation, we use a plausible *a priori* value for the rate of foliar respiration, and test how sensitive the GEP-versus-DER partitioning results are to this value. We find that the choice of *a priori* value, within plausible bounds, is inconsequential for the values of GEP and DER output by IFP (Extended Data Fig. 6), as was also found previously[8]. The partitioning of NEE into GEP and DER is thus robust even if IFP's internal foliar/non-foliar apportioning is not. The plausible bounds for daytime foliar respiration are approximately: (1) zero, and (2) the total night-time aboveground respiration, which was determined by a multiyear synthesis of flux tower and soil chamber data in the typical flux tower sampling footprint at this site[19]. For the partitioning in the main text, we set the *a priori* value in the middle of the range; that is, for each daytime flux measurement, we calculated leaf respiration as $0.5 \times p \times$ NER, where NER is night-time ecosystem respiration (that is, night-time NEE) for the same wind direction, and p is the (seasonally varying) proportion of NER that is aboveground respiration according to the multiyear synthesis mentioned above. In this case, Extended Data Fig. 6 shows that the maximum possible associated error in GEP at any time of the growing season is 3.5%. Given the insensitivity of GEP and DER to the *a priori* rate of foliar respiration, and given that the consideration of foliar respiration in the main text is based on comparison of DER to other kinds of measurement rather than on IFP's internal apportioning, the *a priori* rate of foliar respiration does not affect our findings concerning the inhibition of foliar respiration (or any other findings).

With a measured signature of non-foliar respiration and an *a priori* rate of foliar respiration, the other six variables can be determined simultaneously by solution of the six equations. The equations neglect variation among the leaves within the canopy with regards to physiology and microenvironment, a source of uncertainty in the method that—as we argue in the section 'Uncertainty in the seasonal patterns' (below) and in Extended Data Fig. 7—is unlikely to significantly affect our findings.

Successful application of isotopic partitioning requires that the isotopic signatures of GEP and DER be distinct (otherwise the partitioning equations above are not independent). That is the case predominantly because of the large (4‰) diurnal variation in the signature of GEP and the small (<0.25‰) diurnal variation in the signature of DER. But we also see consistently distinct signatures even at seasonal timescales averaged over three years (Extended Data Fig. 2).

A minor alteration to the previous method[8], enabled by our larger data set here (three growing seasons instead of one), concerns the empirical function used to interpolate eddy-covariance-based estimates of stomatal conductance into periods with significant evaporation (for example, from the soil surface), which would otherwise contaminate the stomatal conductance estimation because it is a water flux that does not pass through the stomata. Previously[8], only one year of data was used. Here the function was fit using all three years of available data, and the resulting set of fitted parameters was still able to closely reproduce the measured half-hourly water flux ($r^2 = 0.92$) in selected evaporation-free periods[8] that we used for testing the method. The strong ability to reproduce the water flux gives us high confidence that stomatal conductance values are well estimated during evaporative periods, and that IFP can therefore be extended to these times.

Note that some parameters used for isotopic partitioning (for example, mesophyll conductance) might be inaccurate during periods of leaf expansion (that is, increase in leaf area following budburst) or autumnal senescence (that is, coloration and abscission), shown as hatched areas in Fig. 2 and Extended Data Figs. 2 and 5–10.

Standard partitioning. For comparisons, we followed the standard partitioning algorithms exactly as described[13,14], except that we used slightly longer time windows for building regressions in order to substantially reduce the number of regressions that were based on only a few data points (we used 6-day windows where 4-day windows were prescribed, and 15-day windows where either 12- or 15-day windows were prescribed). All partitioning methods partitioned the same set of NEE measurements.

Sampling biases in standard partitioning. There are two competing sampling biases in the standard partitioning method used in the main text[13], both of which are related to the fact that both night-time and daytime ecosystem respiration

(the latter as determined by IFP) were more than two times higher in areas to the northwest of the flux measurement tower than they were to the southwest[8] (GEP from IFP was also higher to the northwest, by 28%). The Harvard Forest is not odd in this regard; directional variation in the flux measured by eddy covariance can result from true ecosystem heterogeneity or from correlation of environmental conditions with wind direction, caused by synoptic weather patterns.

The first and larger bias arises because the standard method calculates DER from all night-time flux measurements in a 4- or 6-day time window; thus standard partitioning of a given flux measurement, corresponding to a given wind direction, is influenced by fluxes from many wind directions. This bias leads the standard method to overestimate DER in the southwest quadrant and underestimate it in the northwest quadrant; however, the bias is negligible if estimates of DER from all quadrants are averaged (as in Fig. 2). Restricting the standard partitioning method to use night-time fluxes from only one quadrant in its regressions would require expansion of the time window to almost a month in order to maintain sufficient points for each regression, which would raise concerns about seasonal variation biasing the method[13]. The isotopic method, on the other hand, partitions each flux measurement independently and thereby captures the variation of DER and GEP between different areas of the forest[8].

The second bias arises because natural wind patterns caused the night-time and daytime fluxes to be associated with different areas of the forest. In particular, in June and July (but not in August or September), the high-respiration areas to the northwest were sampled commonly during the daytime but rarely at night. This bias leads the standard method to underestimate DER in June and July but not in August or September. Following the discrepancy between night-time NEE and DER from IFP, the standard partitioning method should overestimate DER from IFP by about 100% in June–July. Instead, when estimates of DER from all quadrants are averaged to remove the first and larger bias (discussed above), this second bias reduces that overestimation to about 35%. If our forest were more homogeneous, the standard method would have overestimated DER by about 100%.

We include all quadrants in the averages in Fig. 2 because it is focused on comparing the two partitioning methods, and the second bias is smaller than the first. On the other hand, we restrict Figs. 1 and 3 to the relatively homogeneous southwest quadrant because they are focused on the day–night difference in respiration and on the light-response of GEP, which are more accurately portrayed without the variability associated with sampling different quadrants.

Standard partitioning adjusted for 100% inhibition of aboveground respiration by light. The dashed blue lines in Fig. 2 were obtained by scaling DER from standard partitioning by the seasonally varying ratio of belowground respiration to total ecosystem respiration in ref. 19, which was estimated from soil chambers and night-time NEE.

Comparison with partitioning based on light-response curves. Regression-based partitioning incorporating a photosynthetic light-response function in addition to a respiratory temperature-response function[14], like the standard regression-based method discussed in the text[13], overestimated DER from IFP in July; however, it diverged from IFP and the more standard method at other times of the year (Extended Data Fig. 8). At this site, there is large horizontal variation in ecosystem respiration, so that changes in the flux tower sampling footprint (that is, in wind speed or direction) can cause the measured respiration to vary by a factor of 3 or more[8]. The dual-function method can only interpret such variation as being driven by PAR, sometimes leading to unrealistic light-response curves and erratic results[8]; examples are evident in August and October in Extended Data Fig. 8. Also like the standard method discussed in the text, dual-function partitioning yielded a light-use efficiency that showed no significant correlation with APAR on the seasonal scale ($r^2 = 0.01$, $P = 0.85$) (Extended Data Figs. 3 and 8), although it did correlate with APAR on shorter timescales (Extended Data Fig. 9).

Uncertainty in the seasonal patterns. Because the estimated systematic uncertainty in IFP at this site exceeds 17% of GEP[8] (1 standard error), we examined the potential for errors in IFP to produce the observed seasonal pattern of disagreement with standard partitioning. The two largest sources of uncertainty in IFP—the only two that could account for a 10% error in GEP[8] in the period after leaf expansion and before senescence—are: (1) neglect of heterogeneity among the canopy leaves and their microenvironments, that is, the 'big-leaf' assumption, and (2) the prescribed isotopic fractionation by enzyme-catalysed fixation of CO_2, which is based on measurements in only a few non-forest species.

Error owing to the big-leaf assumption would depend on the physical and physiological structure of the canopy and on the distribution of the light source (that is, the angle of the sun and the diffuse light fraction). Because the canopy structure does not vary appreciably between full leaf expansion and the onset of senescence, we can minimize any error owing to the big-leaf assumption during that period by restricting our analysis to data acquired under fully diffuse light—that is, when the light source was distributed uniformly over the sky. We found that the seasonal pattern of the disagreement between IFP and standard partitioning is not qualitatively changed by restricting the analysis to fully diffuse light conditions (diffuse light fraction >0.9), or by systematic error in the isotopic fractionation by enzyme-catalysed fixation of CO_2 (aside from a shift in the mean disagreement; Extended Data Fig. 7). Thus the seasonal pattern of disagreement between IFP and standard partitioning is unlikely to be an artefact of uncertainty in IFP.

Random errors. The standard error bands in Figs. 2 and 3 are based on total variability within each averaging bin and therefore represent an upper bound on the effect of random measurement error. The random error in the isotopic partitioning of individual NEE measurements has previously been shown[8] to be negligible compared with the random error in the eddy covariance measurement of NEE itself.

Ogée *et al.*[39] once argued, using Bayesian methods, that even with improved instrumentation, the random error in isotopic partitioning using ^{13}C would remain so large that the partitioning would be useful only when averaging over many individual flux measurements. The rationale for the large error estimate was that the typical isotopic disequilibrium (~2‰) is not much larger than the random measurement error in the isotopic signatures of photosynthesis and respiration, and in the isotopic composition of NEE. However, Ogée *et al.*'s analysis did not account for correlations between the errors in these various isotopic quantities. Because the photosynthetic signature is determined by the partitioning equations (as opposed to being measured), random error in the photosynthetic signature derives entirely from, and is therefore correlated with, random error in the measured variables (especially in the isotopic composition of NEE). That correlation reduces the measurement-derived random error in DER and GEP relative to Ogée *et al.*'s estimates[39], as confirmed by the actual variability in the retrieved gross fluxes not only here but also in all previous IFP studies[31–39]. That variability demonstrates that ^{13}C measurements are sufficiently precise to partition NEE measurements robustly on an hourly basis.

The effect of error in the isotopic composition of NEE on error in the photosynthetic signature using our equations was determined by sensitivity analysis and shown in Fig. 9 of ref. 8, as was the relative insensitivity of GEP to error in the isotopic composition of NEE and other measured variables.

Comparison with other methods for estimating GEP. There are other methods being developed for estimating GEP, including those based on measurements of carbonyl sulfide (OCS), whose uptake by plants has been taken as an index of photosynthetic CO_2 assimilation[40], and of sun-induced chlorophyll fluorescence (SIF)[41], which is correlated with leaf photochemistry. Both OCS and SIF have been measured by others at or near this site for part of the period studied here (Extended Data Fig. 10). However, there are issues with both OCS and SIF that currently prevent these promising methods from estimating the seasonal pattern of GEP at the 5% uncertainty level needed to corroborate our present results. In the case of OCS, one issue is the occurrence of large unexplained emission of OCS at this site[40] (Extended Data Fig. 10). Another is that the uptake of OCS depends on stomatal conductance and carbonic anhydrase content, not on photosynthesis directly[40]. In the case of SIF, the SIF–GEP relationship depends on the degree to which light is limiting photosynthesis (which depends on plant stress and carboxylation capacity)[42] as well as on the proportion of sunlit and shaded leaves seen by the SIF sensor[41], which varies with sun angle, diffuse light fraction, and canopy structure.

29. Goulden, M. L., Munger, J. W., Fan, S.-M., Daube, B. C. & Wofsy, S. C. Measurements of carbon sequestration by long-term eddy covariance: methods and a critical evaluation of accuracy. *Glob. Change Biol.* **2,** 169–182 (1996).
30. Yakir, D. & Wang, X. Fluxes of CO_2 and water between terrestrial vegetation and the atmosphere estimated from isotope measurements. *Nature* **380,** 515–517 (1996).
31. Bowling, D. R., Tans, P. P. & Monson, R. K. Partitioning net ecosystem carbon exchange with isotopic fluxes of CO_2. *Glob. Change Biol.* **7,** 127–145 (2001).
32. Ogée, J. *et al.* Partitioning net ecosystem carbon exchange into net assimilation and respiration using $^{13}CO_2$ measurements: a cost-effective sampling strategy. *Glob. Biogeochem. Cycles* **17,** 1070 (2003).
33. Lai, C.-T., Schauer, A. J., Owensby, C., Ham, J. M. & Ehleringer, J. R. Isotopic air sampling in a tallgrass prairie to partition net ecosystem CO_2 exchange. *J. Geophys. Res.* **108,** 4566 (2003).
34. Knohl, A. & Buchmann, N. Partitioning the net CO_2 flux of a deciduous forest into respiration and assimilation using stable carbon isotopes. *Global Biogeochem. Cycles* **19,** GB4008 (2005).
35. Zhang, J., Griffis, T. J. & Baker, J. M. Using continuous stable isotope measurements to partition net ecosystem CO_2 exchange. *Plant Cell Environ.* **29,** 483–496 (2006).
36. Zobitz, J. M., Burns, S. P., Reichstein, M. & Bowling, D. R. Partitioning net ecosystem carbon exchange and the carbon isotopic disequilibrium in a subalpine forest. *Glob. Change Biol.* **14,** 1785–1800 (2008).

37. Billmark, K. A. & Griffis, T. J. in *Phenology of Ecosystem Processes* 143–166 (Springer, 2009).
38. Fassbinder, J. J., Griffis, T. J. & Baker, J. M. Evaluation of carbon isotope flux partitioning theory under simplified and controlled environmental conditions. *Agric. For. Meteorol.* **153,** 154–164 (2012).
39. Ogée, J. *et al.* Partitioning net ecosystem carbon exchange into net assimilation and respiration with canopy-scale isotopic measurements: an error propagation analysis with $^{13}CO_2$ and $CO^{18}O$ data. *Global Biogeochem. Cycles* **18,** GB2019 (2004).
40. Commane, R. *et al.* Seasonal fluxes of carbonyl sulfide in a mid-latitude forest. *Proc. Natl. Acad. Sci. USA* **112,** 14162–14167 (2015).
41. Yang, X. *et al.* Solar–induced chlorophyll fluorescence that correlates with canopy photosynthesis on diurnal and seasonal scales in a temperate deciduous forest. *Geophys. Res. Lett.* **42,** http://dx.doi.org/10.1002/2015GL063201 (2015).
42. van der Tol, C., Berry, J. A. & Campbell, P. Models of fluorescence and photosynthesis for interpreting measurements of solar–induced chlorophyll fluorescence. *J. Geophys. Res. Biogeosci*. **119,** http://dx.doi.org/10.1002/2014JG002713 (2014).
43. Gatz, D. F. & Smith, L. The standard error of a weighted mean concentration—I. Bootstrapping vs other methods. *Atmos. Environ.* **29,** 1185–1193 (1995).

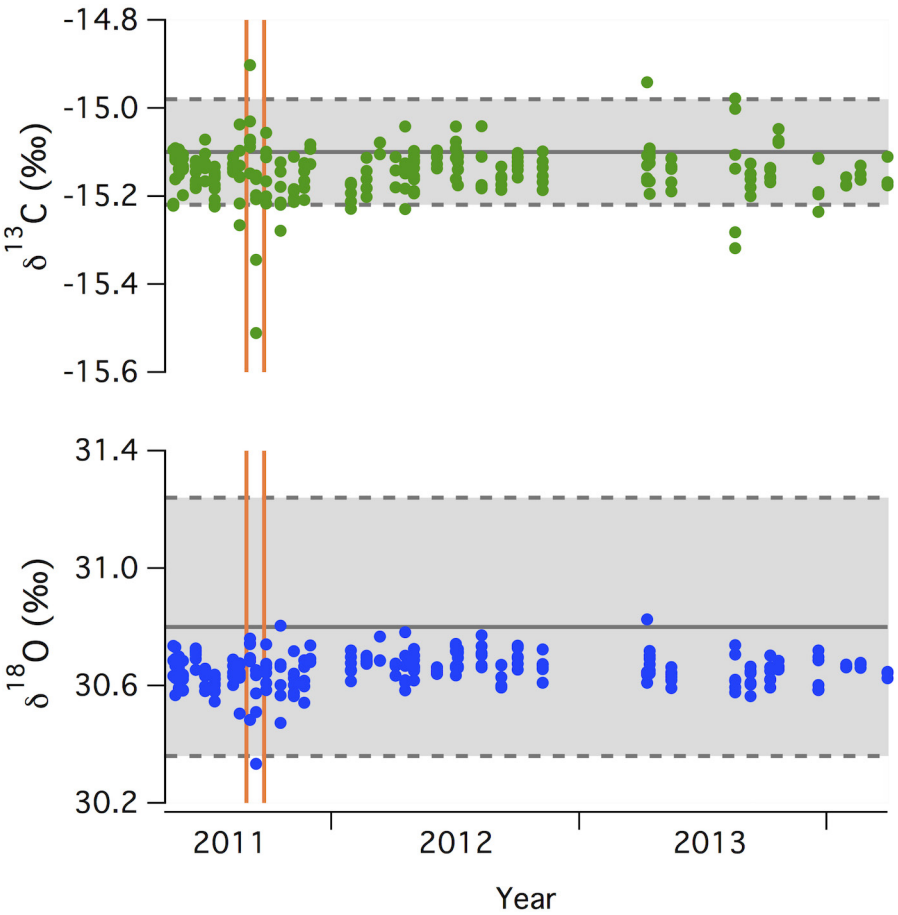

Extended Data Figure 1 | Accuracy and precision of long-term isotopic measurements. Repeated quantum cascade laser spectrometer measurements (dots, each representing a measurement integrated over 100 s) of the isotopic compositions of $\delta^{13}C$ and $\delta^{18}O$ in a single known reference cylinder, but measured as if it were an unknown value interspersed among the three years of routine atmospheric measurements. Known reference cylinder values are indicated by the solid grey lines, with 95% confidence intervals indicated by the grey regions. Except for a period in September 2011 (between the vertical orange lines) when an inferior instrument thermal regulation scheme was tested, the precision of the spectrometer's rapid, *in situ* isotope measurements is seen to be better than that obtained for the reference cylinder by laboratory-based isotope ratio mass spectrometry[7].

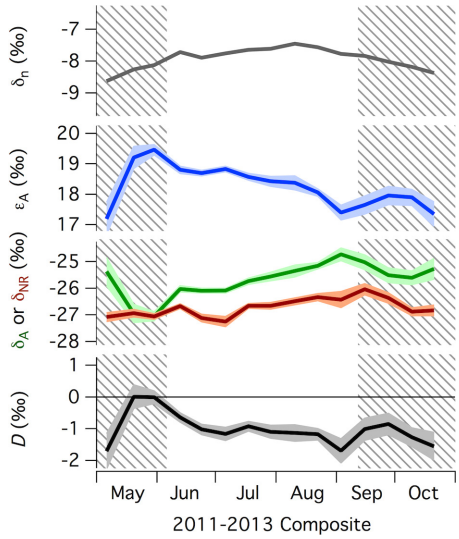

Extended Data Figure 2 | Composite seasonal cycles of isotopic compositions, isotopic discrimination and isotopic disequilibrium. Shown are: the isotopic composition of CO_2 in the canopy airspace, δ_n; the apparent fractionation by net photosynthetic assimilation (also called discrimination), ε_A; the isotopic signatures of net photosynthetic assimilation, δ_A, and non-foliar respiration, δ_{NR}; and the isotopic disequilibrium, $D = \delta_{NR} - \delta_A$. Dark lines connect flux-weighted means over all daylight hours for each 12-day bin, except in the case of δ_{NR}, where the lines connect simple means over all night-time hours for each bin (because δ_{NR} is derived from night-time Keeling plots rather than daytime flux measurements). Light shaded bands show standard errors in the flux-weighted means, calculated according to the ratio variance approximation recommended in ref. 43 (or just standard errors in the means for δ_{NR}), and based on variability within each bin ($64 \leq n \leq 431$ for daylight bins, and $16 \leq n \leq 33$ for δ_{NR}). Hatched areas indicate periods of leaf expansion and abscission.

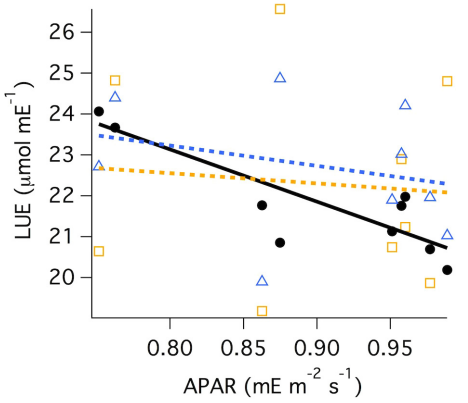

Isotopic Partitioning
r^2 = 0.75; p = 0.003
intercept = 33.4 ± 2.5; slope = -12.8 ± 2.8

Partitioning from Ref. 13
r^2 = 0.07; p = 0.48
interecept = 27.2 ± 6.0; slope = -5.0 ± 6.6

Partitioning from Ref. 14
r^2 = 0.01; p = 0.82
intercept = 24.5 ± 9.6; slope = -2.5 ± 10.7

Extended Data Figure 3 | Relationships of LUE to APAR, from our isotopic partitioning and from both standard methods. Scatterplot of the LUE and APAR data from Fig. 2c (solid black circles), along with ordinary least-squares linear fits (black lines), for the period from full leaf expansion to the onset of senescence. These results are from partitioning based on isotopes. Also shown are results from the standard method of ref. 13 (hollow blue triangles), and from the partitioning method of ref. 14 (hollow yellow squares).

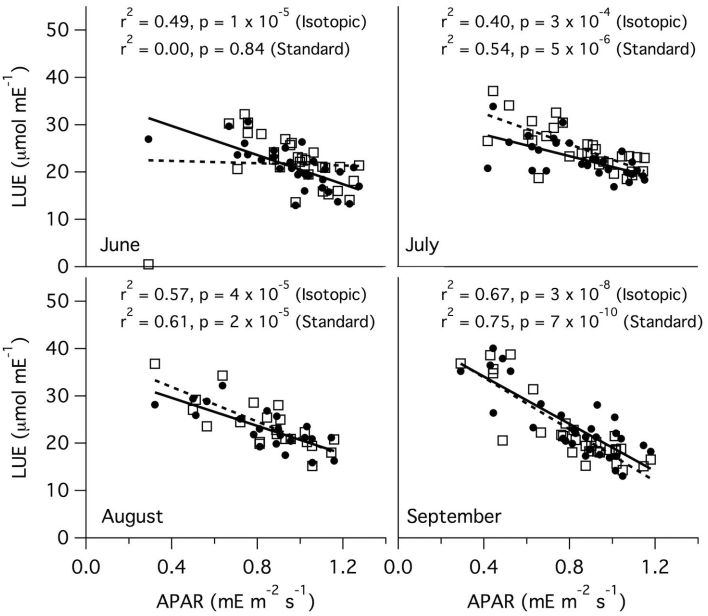

Extended Data Figure 4 | Relationships of LUE to APAR within each month. Daily LUE is plotted against daily APAR, averaged by day of year across all three years, on the basis of isotopic partitioning (solid circles) and the standard method of ref. 13 (hollow squares), and plotted separately for June, July, August and September. Also shown are linear (ordinary least-squares) fits for the isotopic (solid line) and standard (dotted line) partitioning methods.

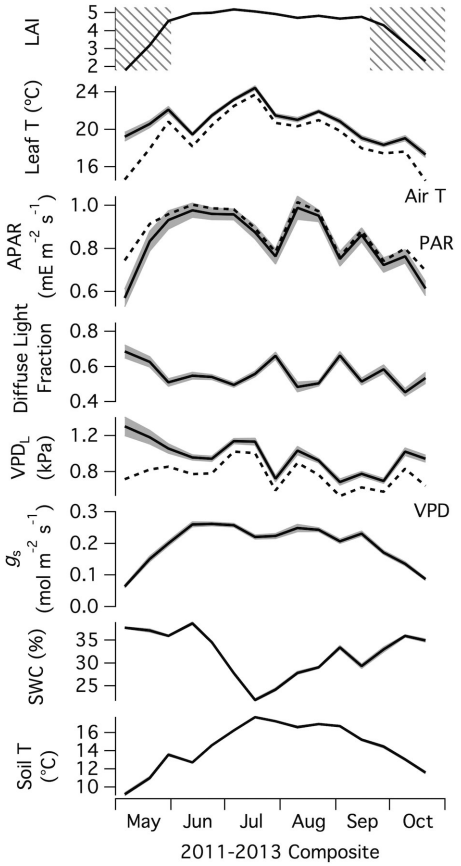

Extended Data Figure 5 | Composite seasonal cycles of environmental variables. Shown are leaf area index (LAI), leaf temperature (Leaf T), APAR, diffuse light fraction, leaf–air water vapour pressure difference (VPD_L), canopy stomatal conductance (g_s), volumetric soil water content (SWC), and soil temperature at 10 cm depth (Soil T), averaged across the three years, 2011–2013. Lines connect means over all daylight hours within each 12-day bin, and grey bands show standard errors in the means, calculated from variability within each bin ($64 \leq n \leq 431$). Air temperature (Air T), PAR, and the atmospheric water vapour pressure deficit (VPD) are also shown, as dotted lines. Hatched areas indicate leaf expansion and abscission.

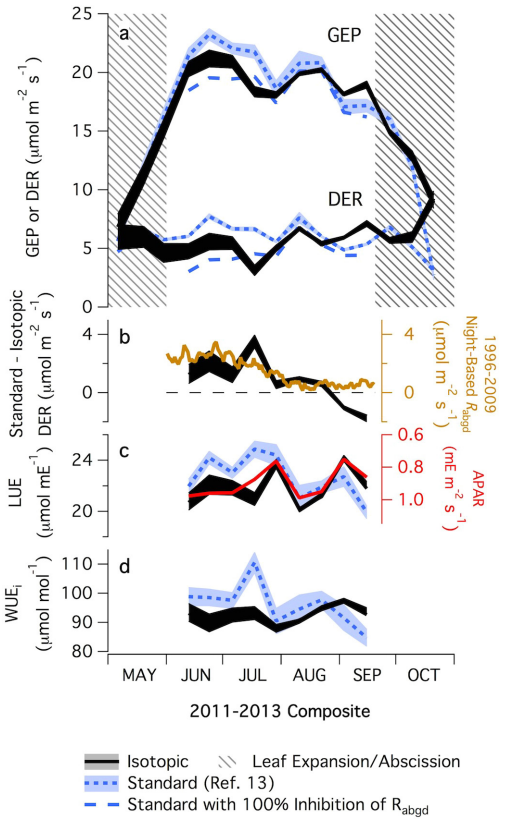

Extended Data Figure 6 | Effect of varying the prescribed rate of foliar respiration on the seasonal patterns of GEP and DER. As for Fig. 2, but with the black lines thickened to show the range of GEP and DER values that result from prescribing between 0% and 100% inhibition of leaf respiration by light. The grey standard error bands in Fig. 2 have been removed here for clarity. Hatched areas indicate leaf expansion and abscission. **a**, GEP and DER. **b**, Discrepancy between standard and isotopic partitioning (black line), with the gold line showing the 1996–2009 mean seasonal pattern of aboveground respiration (R_{abgd}) estimated from soil chambers and night-time NEE[19]. **c**, Light-use efficiency (LUE; isotopic and standard partitioning), with absorbed photosynthetically active radiation (APAR) inverted in red. **d**, Intrinsic water-use efficiency (WUE_i).

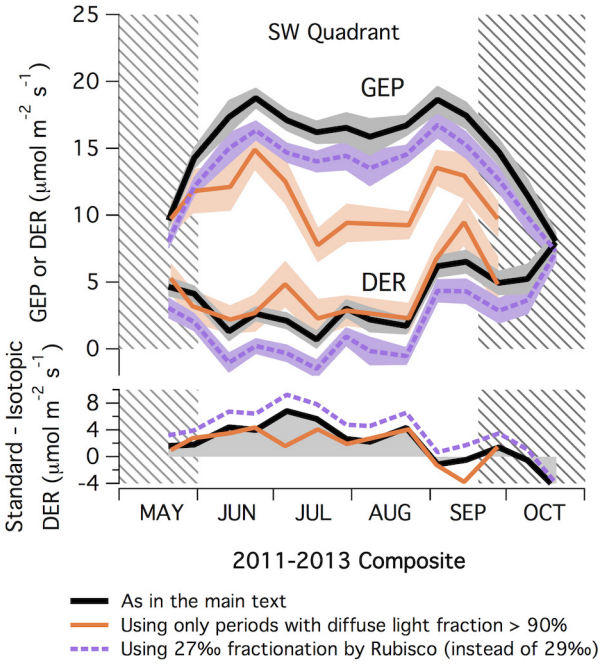

Extended Data Figure 7 | Sensitivity of the seasonal cycles of GEP and DER to change in the isotopic fractionation by the photosynthetic enzyme Rubisco, and to restriction to diffuse light conditions. This figure compares the composite seasonal cycles (across the three years, 2011–2013) of GEP and DER obtained from three variations of the IFP method (restricted to the southwest quadrant to reduce spurious discrepancies caused by differences in the flux tower sampling footprint when subsampling for diffuse light fraction). Top panel: GEP and DER from IFP. Bottom panel: the discrepancy between values of DER obtained from standard partitioning (based on night-time NEE and temperature), and values obtained from isotopic partitioning. The IFP variations shown are: as described in the text (solid black lines); restricted to periods with diffuse light fractions greater than 90% (solid orange lines); and using 27‰ instead of 29‰ for the isotopic fractionation by Rubisco-catalysed fixation of CO_2 (dotted purple lines). The lines connect the means (which are from all daylight hours) for each 12-day bin. The light shaded bands around each line in the top panel show the standard error of the mean, calculated from the variability within each bin ($25 \leq n \leq 130$). Hatched areas indicate periods of leaf expansion and abscission.

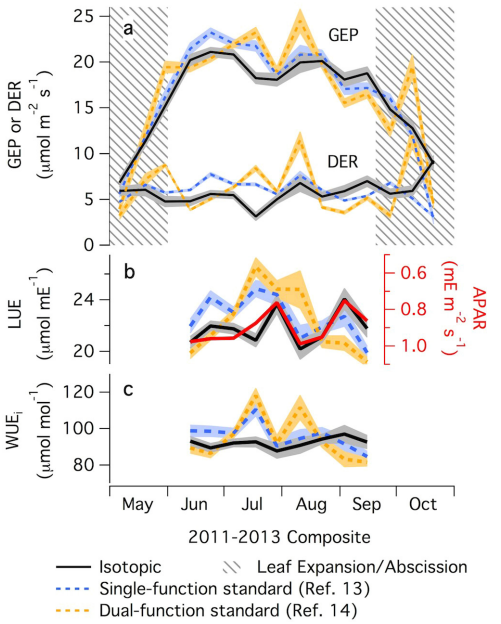

Extended Data Figure 8 | Composite seasonal cycles, from isotopic partitioning and from both standard partitioning methods. Shown are results from isotopic partitioning (solid black); from standard partitioning based on night-time NEE and temperature (dotted blue); and from standard partitioning incorporating a photosynthetic function of light (dotted yellow). **a**, GEP and DER. **b**, LUE, with APAR inverted in red. **c**, WUE_i. Lines connect means over all daylight hours for each 12-day bin; pale bands show standard errors of the means calculated from variability within each bin ($64 \leq n \leq 431$).

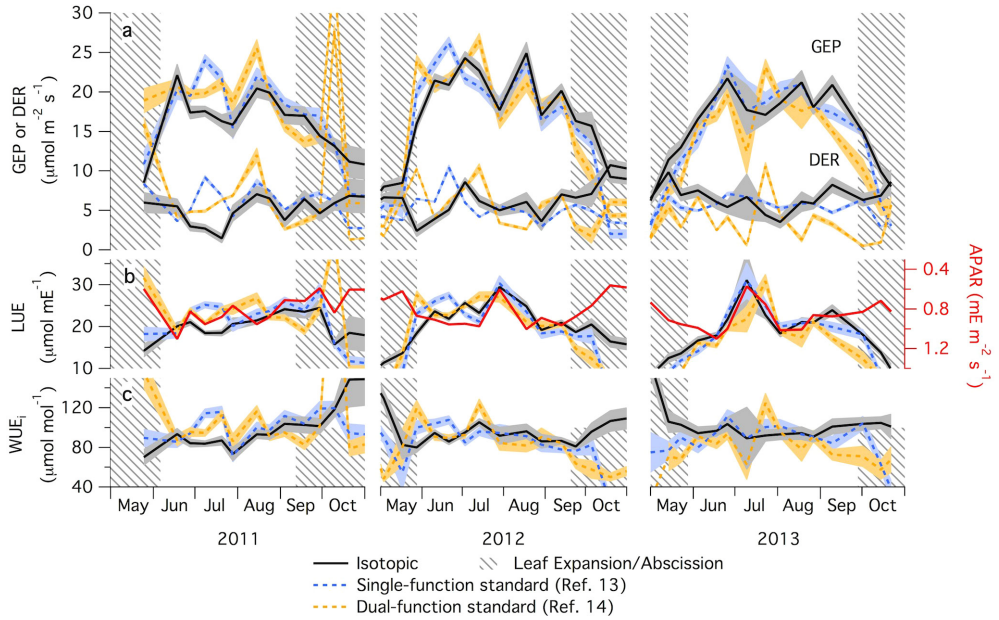

Extended Data Figure 9 | Seasonal cycles from isotopic partitioning and from both standard partitioning methods, for individual years. As for Extended Data Fig. 8, but showing the individual years separately ($8 \leq n \leq 204$).

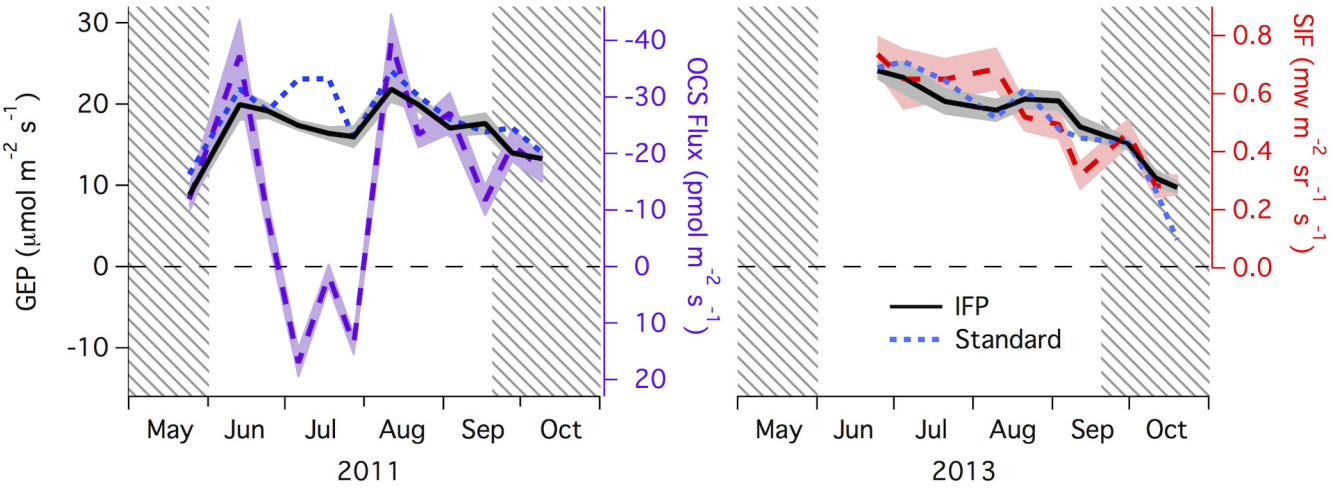

Extended Data Figure 10 | Comparison of GEP values obtained from isotopic partitioning with preliminary estimates based on measurements of carbonyl sulfide and solar-induced fluorescence. Seasonal patterns of GEP from IFP (solid black) and from the standard method of ref. 13 (dotted blue) are compared with those of the OCS flux in 2011 (dashed purple, on an inverted scale) and the SIF signal in 2013 (dashed red). Lines connect means for each 12-day bin, and pale bands show standard errors of the means calculated from variability within each bin ($10 \leq n \leq 209$). The analysis included only data points for which simultaneous GEP and OCS, or GEP and SIF, measurements were available. The OCS data were provided by Commane *et al.*[40], and the SIF data by Yang *et al.*[41].